# A multidisciplinary robust optimisation framework for UAV conceptual design

**N. Van Nguyen**

**J.-W. Lee**
**jwlee@konkuk.ac.kr**

**Y.-D. Lee**

Aerospace Information Engineering Department
Konkuk University
Seoul
South Korea

**H.-U. Park**

Department of Aerospace Engineering
Ryerson University
Toronto
Canada

## ABSTRACT

This paper describes a multidisciplinary robust optimisation framework for UAV conceptual design. An in-house configuration designer system is implemented to generate the full sets of configuration data for a well-developed advanced UAV analysis tool. A fully integrated configuration designer along with the UAV analysis tool ensures that full sets of configuration data are provided simultaneously while the UAV configuration changes during optimisation. The computational strategy for probabilistic analysis is proposed by implementing a central difference method and fitting distribution for a reduced number of Monte Carlo Simulation sampling points. The minimisation of a new robust design objective function helps to enhance the reliability while other UAV performance criteria are satisfied. In addition, the fully integrated process and a probabilistic analysis strategy method demonstrate a reduction in the probability of failure under noise factors without any noticeable increase in design turnaround time. The proposed robust optimisation framework for UAV conceptual design case study yields a more trustworthy prediction of the optimal configuration and is preferable to the traditional deterministic design approach. The high fidelity analysis ANSYS Fluent 13 is performed to demonstrate the accuracy of proposed framework on baseline, deterministic and RDO configuration.

**Paper No. 4058.** Manuscript received 13 August 2013, revised version received 20 November 2013, accepted 21 November 2013.

https://doi.org/10.1017/S0001924000009027 Published online by Cambridge University Press

# NOMENCLATURE

| | |
|---|---|
| $\eta_{prop}$ | propeller efficiency |
| $\sigma_y^2$ | adjusted variance |
| $\sigma_{zi}$ | standard deviation |
| $\mu_y$ | adjusted mean function |
| $\beta$ | propeller pitch angle |
| $\Delta C_{df}$ | increase in drag due to flap deflection |
| $C_L$ | lift coefficient |
| $C_{Lmax}$ | maximum lift coefficient |
| $C_{Do}$ | parasite drag coefficient |
| $C_{Di}$ | induced drag coefficient |
| $C_{l\beta}$ | static lateral derivative |
| $C_{n\beta}$ | static directional derivative |
| $C_{m\alpha}$ | static pitching derivative |
| $C_T$ | thrust coefficient |
| $k$ | induced drag factor |
| J | propeller advanced ratio |
| $L/D$ | lift to drag ratio |
| $R/C$ | rate of climb in $ms^{-1}$ |
| SM | static margin |
| $S_{to}$ | take-off distance in m |
| $S_{land}$ | landing distance in m |
| $S_W$ | wing area in $m^2$ |
| PCT | power setting in percentage |
| $T_{var}$ | target variance |
| $T_{\mu_y}$ | target mean value |
| $V_{stall}$ | stall speed in $ms^{-1}$ |
| $V_{max}$ | maximum speed in $ms^{-1}$ |
| $V_{design}$ | design flight speed in $ms^{-1}$ |
| $W_e$ | empty weight in kg |
| $W_o$ | take-off gross weight in kg |
| MALE | Medium Altitude Long Endurance |
| MCS | Monte Carlo Simulation |
| UAV | Unmanned Aerial Vehicle |
| $z_i$ | noise factors |
| WOT | Wide Open Throttle |

# 1.0 INTRODUCTION

A recent trend in aircraft conceptual design activity is to develop or to implement quick and accurate design analysis tools for seeking deterministic optimal design solutions comprising many complex and highly-coupled subsystems and disciplines[1] with the help of optimisation algorithms. The optimal results from the conceptual design stage play an extremely important role in the next preliminary and detailed design stage. However, the nondeterministic nature of the complex aircraft design problem and the importance of modelling the human designer's

https://doi.org/10.1017/S0001924000009027 Published online by Cambridge University Press

decision-making activities have been largely neglected[2] at the conceptual design stage. For example, the design flight speed is required as a design variable to maximise the aircraft's critical performance features in the conceptual design of Medium Altitude Long Endurance (MALE) UAVs. The design flight speed might be slightly changeable during very long endurance or it might be affected by the wind. In addition, rounding off the main geometry parameters during construction of the mathematical models or the manufacturing stage and a lack of knowledge might lead to variations in the optimal conceptual design solutions. These sources are called uncertainty or unexpected deviations. Robust design is applied to prevent such phenomena[3]. Robust design has been recognised and applied in control system design and structural design as the state-of-the-art for those particular fields. Doltsinis *et al* introduce a robust design framework for a multi-criteria structure design problem in which the sensitivities of the mean values and the variance of the structural performance function according to design variables are calculated in an optimisation task[4]. The robust design is applied to minimise the expected value and standard deviation of the objective function in structure design[4]. Dimitri N. Mavris *et al* implement a Robust Design Simulation (RDS) in high-speed civil transportation to show why a probabilistic approach to aircraft design is preferable to the traditional deterministic approaches[2]. H.U. Park *et al* applied a robust design process for the Very Light Jet (VLJ) design optimisation[5] that improves VLJ performance quality while considering the noise factors of aircraft speed and flight altitude. Wei Chen *et al* apply robust design for improving vehicle handling performance. The proposed process using robust design is effective for preventing the worst manoeuvre conditions and a range of manoeuvre inputs as well[6]. In addition, Wei Chen *et al* present a flexible robust design process to provide more freedom to the discipline that takes the role of follower[7]. Xiaoping Du *et al* evaluated the efficiency of uncertainty analysis methods for multidisciplinary robust design compared with the conventional Monte Carlo simulation approach[8]. The system uncertainty analysis (SUA) method and the concurrent subsystem uncertainty analysis (CSSUA) method are proposed and developed to estimate the mean and variance of system performance subject to uncertainties or noise factors[7] in a multidisciplinary design optimisation (MDO) environment. Robust design is also applied in the structure design problem. Wei Chen *et al* introduces the Response Surface Methodology (RSM) and Decision Support Problem (DSP) for a computationally expensive robust design problem[9]. Eric Sandgren *et al* present an optimal structure design with consideration of load, material properties and geometry uncertainty[10]. The Monte Carlo simulation is embedded with a genetic algorithm for outputs distribution simulation. The optimal structure design shows a better map of the designer's intent[10].

In this study, a MALE UAV is considered as a design application. Several uncertainty parameters affect UAV performance and especially endurance, such as a flight altitude, speed, wind effect and propeller efficiency during the cruise condition. Therefore, the multidisciplinary robust optimisation framework for conceptual design of Unmanned Aerial Vehicles (UAVs) is developed and proposed to enhance the quality of UAV performance results, reducing the sensitivity to performance variations while minimising the effects of the noise factor. The deterministic and robust optimum configurations with probabilistic analysis results are presented to demonstrate the improved robustness and more trustworthy UAV performance compared with the traditional deterministic optimisation approach, which does not consider noise factors.

https://doi.org/10.1017/S0001924000009027 Published online by Cambridge University Press

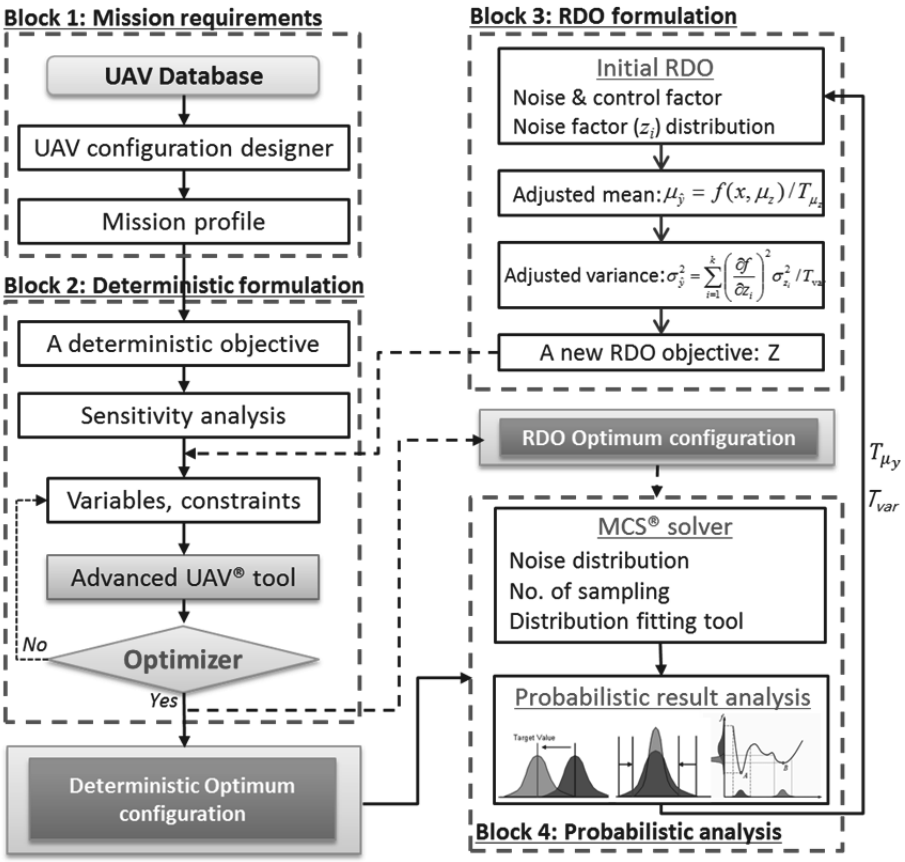



Figure 1. Robust Design Optimisation (RDO) process.

## 2.0 ROBUST DESIGN OPTIMISATION (RDO) FRAMEWORK

The robust design optimisation framework is presented in Fig. 1 and includes mission requirements, deterministic and RDO formulations and a probabilistic analysis block. The RDO framework is developed and integrated using ModelCenter 10.1 software[11] to improve the product's quality and to minimise the effects of noise factors while considering uncertainty parameters in aerospace vehicle design application. The framework starts with mission requirements and deterministic formulation in Block 1 and Block 2, respectively. Then, the analysis and optimiser are implemented to figure out the deterministic and RDO optimum configurations after Block 3 termination. The Monte-Carlo Simulation (MCS solver)[11] is applied to perform a probabilistic analysis for both the deterministic and RDO optimum results in Block 4: Probabilistic analysis. The probabilistic results are analysed to demonstrate the improvement of aircraft performance variability to noise factors compared with the traditional deterministic optimisation approach.

https://doi.org/10.1017/S0001924000009027 Published online by Cambridge University Press

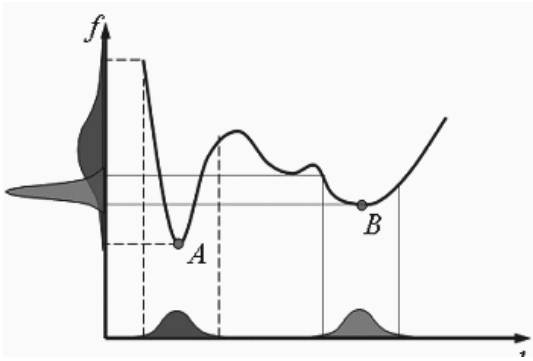



Figure 2. Comparison of two design points in robustness of objective function[12].

## 2.1 Introduction to Robust Design Optimisation (RDO)

Robust Design Optimisation is implemented to substantially reduce the variability of aircraft quality by minimising the effects of uncertainty then removing the source of noise or uncertainty parameter effects on vehicle performance parameters. An example of a robustness result is shown in Fig. 2 in which result point B presents a higher objective value but a lower variance with a more trustworthy and robust result.

## 2.2 Block 1: Mission requirements

The mission requirements are required to specify for UAV design optimisation process. Then, it starts to create a UAV configuration from a database for fuselage, wing, horizontal tail and vertical geometry data by applying an in-house UAV configuration designer[13]. The outputs of the UAV configuration designer provide a full set of configuration data including a fuselage cross-section, wetted area, aerofoil data, horizontal, wing and vertical geometry for the Advanced UAV analysis tool in Block 2, as shown in Fig. 1.

## 2.3 Block 2: Deterministic formulation

The objective function definition must be defined in Block 2 to perform a sensitivity analysis which helps to remove design variables which have a small effect on the selected objective function and other aspects of UAV performance. Then, the deterministic optimum configuration is determined by the help of optimiser and Advanced UAV analysis tool. The deterministic optimum configuration is provided to Block 4: Probabilistic analysis to obtain a mean and variance values by performing MCS solver.

The in-house Advanced UAV tool is an integrated design and analysis tool. It has been developed and validated by the authors for various types of aircrafts such as UAVs and UCAVs[14,15]. The analysis module is composed of the aerodynamics and stability and control, mission, propulsion, weight and performance discipline, as shown in Fig. 3. The Design Explorer algorithm, developed by Boeing and integrated into PHX ModelCenter 10.1[11], helps to search an entire design space using surrogate models with a sequential optimisation algorithm (SEOPT)[16]. The Design Explorer has been implemented and validated in many Boeing design applications such as high lift aerodynamics, multidisciplinary wing planform design, forming of aircraft wing skin, engine duct seal and other products[16]. Therefore, Design Explorer is selected as the optimiser in the framework.

https://doi.org/10.1017/S0001924000009027 Published online by Cambridge University Press

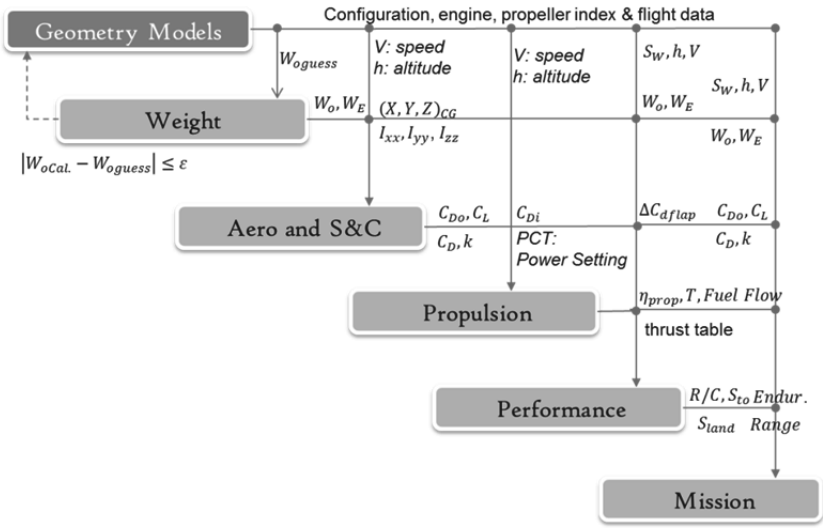



Figure 3. Advanced UAV analysis dataflow.

## 2.4 Block 3: RDO formulation

RDO formulation is to establish a new RDO objective function based on a set of target mean ($T_{\mu_y}$) and target variance ($T_{var}$) values according to noise factors based on the deterministic optimum configuration probabilistic results as shown in Fig. 1. The new RDO objective function ($Z$) is a summation of adjusted mean and variance function. The adjusted mean function consists of noise and a control factor in Equation (1). The adjusted variance is a summation of an objective function differentiation according to noise factors ($z_i$), shown in Equation (2). The new problem is to minimise the new objective function as shown in Equation (3)[12].

$$\text{Adjusted mean value of response:} \quad \mu_{\hat{y}} = f(x, \mu_z) / T_{\mu_y} \qquad \ldots (1)$$

$$\text{Adjusted variance of response:} \quad \sigma^2_{\hat{y}} = \sum_{i=1}^{k} \left( \frac{\partial f}{\partial z_i} \right)^2 \sigma^2_{z_i} / T_{\text{var}} \qquad \ldots (2)$$

$$\text{Minimise:} \quad Z = (\text{adjusted mean value}) + (\text{adjusted variance}) \qquad \ldots (3)$$

The central numerical difference is applied to determine an adjusted variance of response to noise factors, as shown in Equation (2).

## 2.5 Block 4: Probabilistic analysis

Monte Carlo Simulation (MCS) is used for probabilistic analysis of both the deterministic and the RDO optimum configurations, as shown in Fig. 1. The distribution for noise factors is considered and assigned in Block 4 for probabilistic analysis results. The sampling points for MCS are performed on 500, 1,000 and 1,500 sampling runs to estimate the trend of variance and mean value while increasing the sampling runs by implementing the distribution fitting methods. Hence,

https://doi.org/10.1017/S0001924000009027 Published online by Cambridge University Press

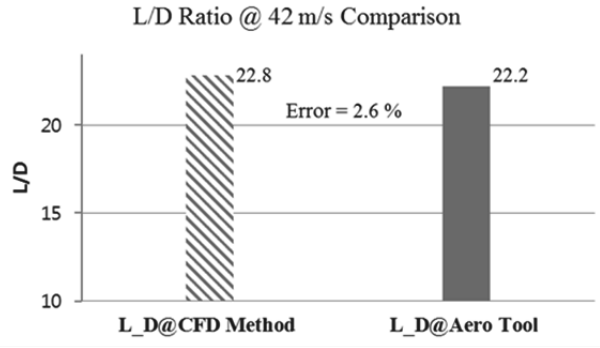



Figure 4. Lift to Drag (*L*/*D*) ratio comparison at speed of 42ms$^{-1}$.

the sampling points for MCS are determined to reduce the computation burden in MCS for both deterministic optimum and RDO configuration results.

# 3.0 VERIFICATION FOR ADVANCED UAV ANALYSIS TOOL

## 3.1 Aerodynamics and S&C analysis module

The Predator A configuration[17] is selected as the baseline for the tool validation. The analysis results from the Advanced UAV analysis tool are compared with the Predator A published data and Computational Fluid Dynamics (CFD) Fluent result[18] in Fig. 4. The *L*/*D* is predicted for the wing only for different angles of attack (AoA). The Predator A reaches *L*/*D* at 22·8 with AoA around 2~3 deg. The *L*/*D* is calculated by using the Advance UAV tool for the whole aircraft at 22·2, as shown in Fig. 4. The slight difference is caused by most of the wing lift contribution on Predator A. The horizontal stabiliser and fuselage make a small contribution to the whole aircraft configuration.

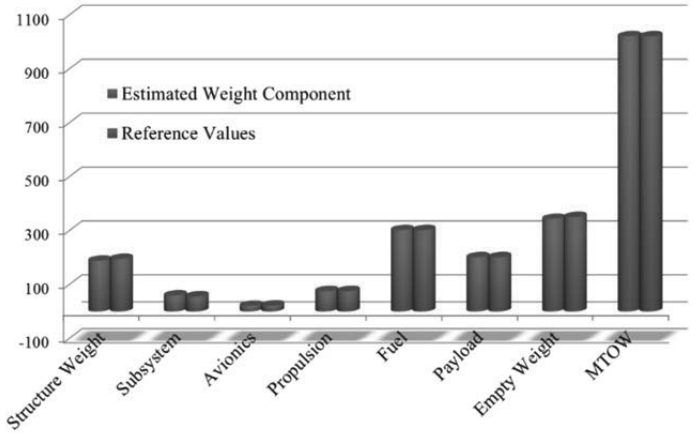



Figure 5. Weight analysis discipline validation.

https://doi.org/10.1017/S0001924000009027 Published online by Cambridge University Press

### 3.2 Weight analysis module

A comparison of the estimated weight components is shown in Fig. 5. The estimated weight components show relatively good agreement with the reference weight component[17], as shown in Table 1. The maximum error is around 6% at the subsystem weight component, while the published empty and weight data for Predator A are 350kg and 1,020kg, respectively. Therefore, it is concluded that the weight analysis module is well-suited for UAV configuration.

**Table 1**
**Weight component comparison for Predator A**

| Estimated Weight (kg) | Reference[17] (kg) | | Error (%) |
|---|---|---|---|
| Avionics | 20·58 | 21·80 | 5·58 |
| Structure Weight | 188·11 | 194·74 | 3·41 |
| Subsystem | 59·08 | 55·60 | 6·26 |
| Empty Weight | 343·28 | 350·17 | 1·97 |
| MTOW | 1,011·70 | 1,020·60 | 0·87 |

### 3.3 Propeller analysis module

Validation of the propeller analysis code is performed on a two-blade propeller[19]. The results show relatively good agreement with the experimental data at three different propeller pitch angles (β) for thrust coefficients versus advanced ratio (*J*).

### 3.4 Performance analysis module

Performance validation is performed on the Predator A configuration as shown in Table 2. The published data is given for detailed take-off, landing condition, and endurance. The comparison results show good agreement with the published data on Predator A. The maximum take-off and landing lift coefficient is assumed to calculate at 25 and 35 degree of flap deflection respectively. The engine is a Rotax Turbo Charge 914[20]. The friction coefficient for the take-off and landing condition including brake are assumed at 0·025 and 0·3 from D. Raymer[21]. The performance validation results show a maximum error of 9·26% for take-off ground roll distance, as shown in

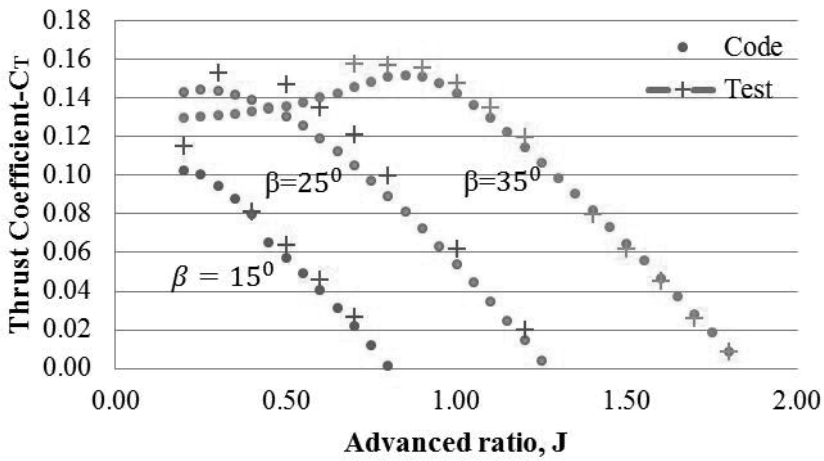



Figure 6. Two-blade propeller analysis validation.

https://doi.org/10.1017/S0001924000009027 Published online by Cambridge University Press

Table 2. The landing and take-off field distance and endurance with a full payload case of Predator A are validated within less than 6·3% error compared with the published data in Table 2 2

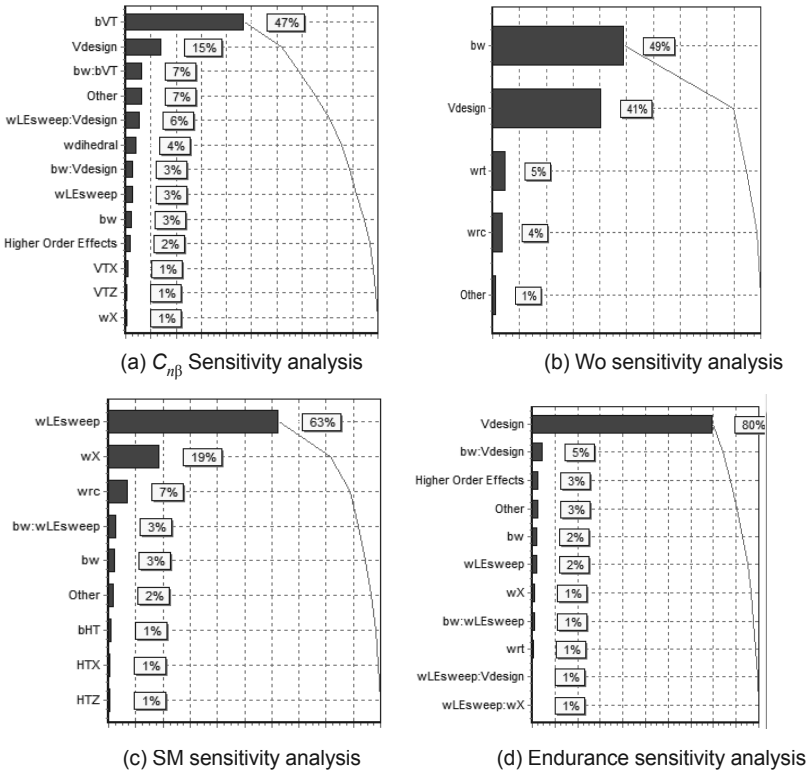
**Table 2**
**Predator A performance validation**

| Performance Parameters | Predator A | Advanced UAV tool | Error (%) | Unit |
|---|---|---|---|---|
| Take-off ground roll | 1,440 | 1,306·59 | 9·26 % | ft |
| Take-off field length (50ft) | 2,000 | 1,922·48 | 3·88 % | ft |
| Landing field length (50ft) | 1,700 | 1,731·82 | 1·87 % | ft |
| Endurance (full payload) | 18 | 18·6 | 3·33 % | hours |

# 4.0 IMPLEMENTATIONS OF RDO FRAMEWORK FOR MULTIDISCIPLINARY UAV DESIGN

## 4.1. Sensitivity analysis

Sensitivity analysis is performed on 21 variables of the MALE UAV configuration including wing, horizontal tail, vertical tail, and their location to 18 constraints and endurance, as shown in Table 4. 500 design points are selected by implementing the Latin Hyper-cube and orthogonal methods[11]




(a) $C_{n\beta}$ Sensitivity analysis (b) Wo sensitivity analysis

(c) SM sensitivity analysis (d) Endurance sensitivity analysis

Figure 7. Sensitivity analysis for a multidisciplinary UAV design.

https://doi.org/10.1017/S0001924000009027 Published online by Cambridge University Press

to execute the Advanced UAV analysis program. Four sensitivity analysis results for directional stability derivatives, gross weight, static margin (SM) and endurance are shown in Fig. 7. The main effects for directional stability derivatives are vertical span (*bVT*), design speed ($V_{design}$) and wing geometry, as shown in Fig. 7(a), which agree with aircraft stability characteristics. Similarly, the main effects for static margin are wing sweep angle (*wSweep*) (63%), wing location (*wX*) and wing root chord (*wrc*), as shown in Fig. 7(b). Wing span (*bw*), design speed ($V_{design}$), wing tip (*wrt*) and wing root (*wrc*) have a major effect on the gross weight due to the small weight contribution of the horizontal and vertical tail, as shown in Fig. 7(c). The endurance parameter is mainly affected by design speed (80%) due to the gross weight being kept a constant for an electric-powered UAV. If UAVs fly at a lower speed, the endurance increases with flight speed. Other effects on endurance are a combination of wing span and speed relating to aerodynamics parameters and other wing geometry parameters, as shown in Fig. 7(c). The higher order effects of the design variables are neglected during the sensitivity analysis.

Therefore, the main effective variables for UAV endurance and 17 constraints are kept as in Table 3 and Table 6. The vertical location of the wing, horizontal and vertical tail are neglected for the design formulation, being slightly affected by endurance and constraints.

## 4.2. MALE UAV design formulation

### 4.2.1 Deterministic optimisation formulation

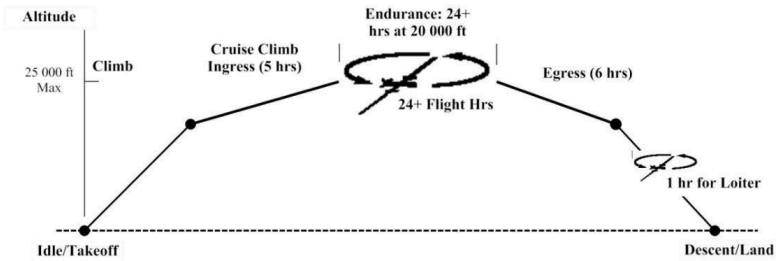



Figure 8. Predator A missile profile[17].

The mission profile of Predator A is shown in Fig. 8. The Predator A design optimisation is performed to increase the endurance time in the cruise flight condition with a full payload condition.

- the climb and ingress is designed for 5 hours.
- egress and descent/land stage is designed for 6 hours.
- loiter time condition is designed for 1 hour.

The design condition is considered at cruise condition with no payload and full payload condition for 18 and 24 hours, respectively[17]. The designed condition is a cruise condition with full payload aimed for Predator A. The 18 design variables including wing, horizontal and vertical tail geometry and flight condition are listed in Table 4 after a sensitivity analysis step.

The endurance of MALE UAVs is a major factor for surveillance and other missions. Therefore, it is selected as an objective function to maximise for MALE UAV.

$$\text{Maximise } Endurance = Endur((x_i)\, j = 1{,}18 \quad \ldots (4)$$

$$\text{Subject to: } \Pi(G_i(X)) > 0,\ \ i = 1,\ldots,17 \quad \ldots (5)$$

https://doi.org/10.1017/S0001924000009027 Published online by Cambridge University Press

**Table 3**
**Design variables for multidisciplinary UAV design optimisation**

| | Baseline | Lower Bounds | Upper Bounds | Unit |
|---|---|---|---|---|
| Wing span | 14·8 | 10 | 20 | m |
| Wing root chord | 1·24 | 1·0 | 1·4 | m |
| Wing tip chord | 0·5 | 0·3 | 0·7 | m |
| Wing sweep | 5 | 0 | 10 | deg |
| Wing dihedral | 0 | 0 | 5 | deg |
| Wing X location | 3·59 | 3 | 4 | m |
| HT span | 4 | 3·5 | 4·5 | m |
| HT root chord | 0·742 | 0·4 | 1 | m |
| HT tip chord | 0·742 | 0·4 | 1 | m |
| HT sweep | 0 | 0 | 10 | deg |
| HT X location | 6·82 | 5·8 | 7·8 | m |
| VT span | 1·14 | 0·7 | 1·5 | m |
| VT tip chord | 0·742 | 0·4 | 1 | m |
| VT root chord | 0·742 | 0·4 | 1 | m |
| VT LE sweep | 0 | 0 | 60 | deg |
| VT X location | 6·82 | 5·8 | 7·8 | m |
| $V_{design}$ | 42 | 27·78 ($V_{stall}$) | 64 | $ms^{-1}$ |
| $h$ | 3,000 | 2,000 | 4,000 | m |

**Table 4**
**Design constraints for multidisciplinary UAV design optimisation**

| Constraints | Description | Discipline |
|---|---|---|
| G(1,2) | Static margin: 0·05 ≤ SM ≤ 0·2 | S&C (@$V_{design}$) |
| G(3) | Take-off field length ≤ 700 (m) (2,300ft) | Perf (50ft) (WOT) |
| G(4) | Lateral stability derivative: $C_{l\beta} \leq -0{\cdot}03$ | S&C (@$V_{design}$) |
| G(5) | Gross weight: MTOW ≤ 1,020kg | Weight |
| G(6) | Pitching moment der· $C_{ma} \leq 0$ | S&C (@$V_{design}$) |
| G(7) | Landing distance ≤ 518m 1,700ft | Perf· |
| G(8) | Wing weight: Wwing ≤ $W_{baseline}$ (kg) | Weight |
| G(9) | Lift over drag ratio: $L/D \geq L/D_{baseline}$ | Aeros (@$V_{design}$) |
| G(10) | Wing taper ≥ 0·4 | Geometry |
| G(11) | Take-off ground roll ≤ 438m (1,440ft) | Perf (@WOT) |
| G(12) | Maximum speed ($V_{max}$) ≥ 60·3$ms^{-1}$ | Perf (@WOT) |
| G(13) | Stall speed ($V_{stall}$) ≤ 27·8$ms^{-1}$ | Perf (Clean) |
| G(14) | Service ceiling ≥ 25,000ft | Perf (@WOT) |
| G(15,16) | Directional derivatives coefficient 0·08 ≤ $C_{n\beta} \leq 0{\cdot}28$ | S&C (@$V_{design}$) |
| G(17) | Empty weight: We ≤ We_Baseline(kg) | Weight |

https://doi.org/10.1017/S0001924000009027 Published online by Cambridge University Press

#### 4.2.2 RDO formulation

The altitude ($h$) and flight speed ($V$) are considered as noise factors for the MALE UAV cruise design condition. The adjusted variance function is calculated by implementing a central difference method as in Equation (6).

$$\sigma_y^2 = \left[ \left( \frac{f(V+\Delta V) - f(V-\Delta V)}{2\Delta V} \right)^2 + \left( \frac{f(h+\Delta h) - f(h-\Delta h)}{2\Delta h} \right)^2 \right] \times \left( \frac{1}{3} \right)^2 \times \frac{1}{T_{\text{var}}} \quad \ldots (6)$$

where $\Delta V$ and $\Delta h$ are flight speed and altitude step.

A new objective function for RDO is defined by Equation (3) with the altitude and speed noise factors considered in Equation (6).

### 4.3. Deterministic and robust design optimum results

#### 4.3.1 Deterministic optimum configuration and MCS results

The deterministic optimum configuration results are shown in Table 5. The MCS are performed on the deterministic optimum configuration for 500, 1,000 and 1,500 sampling points, then the distribution fitting tool (dfittool)[22] is performed to evaluate the effective number of sampling points for UAV conceptual design framework. The results are shown in Fig. 9 and Table 5 by using the distribution fitting tool. The mean and variance value are estimated from the fitting model in Table 5 in which the difference between 1,000 and 1,500 sampling points are approximately 0·026% for mean and variance value. In addition, the 1,500 sampling points fitting curve is most overlapped on 1,000 sampling points in Fig. 9. Therefore, the 1,500 sampling points are selected to perform MCS, then the distribution fitting tool is implemented to determine the mean and variance value for next RDO optimum configuration MCS results. The MCS and fitting distribution tool strategy helps to reduce the huge computational load during MCS.

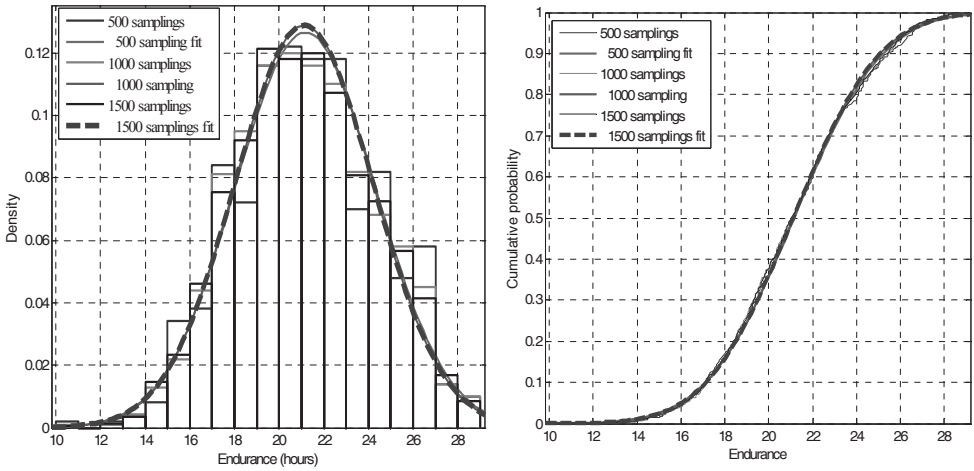
**Table 5**
**Deterministic MCS fitting results comparison for different sampling points**

| Monte Carlo Simulation | Mean value | Variance value |
|---|---|---|
| 500 sampling points | 21·17 | 9·95 |
| 1,000 sampling points | 21·118 | 9·5943 |
| 1,500 sampling points | 21·1125 | 9·5951 |

#### 4.3.2 Deterministic and RDO optimum results comparison

The deterministic and robust design optimum configuration results for multidisciplinary UAV design optimisation are presented in Table 6 compared with a baseline Predator A configuration. The endurance objective function shows an improvement in both the deterministic and RDO UAV results from 18·6 hours to 21·13 and 22·26 hours for the deterministic and robust design results respectively, with the help of the Design Explorer algorithm. The objective convergent history and maximum violation constraints for a deterministic formulation are shown in Fig. 9. The endurance objective function converges at 21·13 hours with 1% constraints violation in Fig. 9(b). The new objective function for RDO includes an adjusted endurance mean function and adjusted variance which converges to 1 with no constraints violation, as shown in Figs 10(a) and 10(b). The wing weight and directional derivatives coefficient constraints are active. Hence, the design formulation

https://doi.org/10.1017/S0001924000009027 Published online by Cambridge University Press




(a) Normal distribution probability (b) Cumulative probability

Figure 9. Deterministic MCS and fitting results for 500, 1,000 and 1,500 sampling points.

problems for the deterministic and robust design processes converge and are strictly formulated. The maximum constraints violation graphs also show that if designers accept more risk in constraints violation, the endurance objective value is also increased as shown in Figs 9(b) and 10(b).

The wing span in RDO optimum configuration is shorter than a baseline and deterministic optimum configuration which is able to fly with minimising a speed and altitude uncertainty effects on the UAV endurance. The shorter wing span drives to a smaller lift to drag ratio in RDO configuration. However, the endurance shows in improvement in the RDO configuration for a robust configuration. Because, the speed is reduced to $36{\cdot}8 ms^{-1}$ which adjust a smaller fuel flow burned during flight. In addition, the flight altitude is lower than a baseline at 2,025m comparing with 3,000m of baseline. Therefore, it provides more air density and lift force to maintain lift to drag ratio constraints. The static margin (SM) of RDO configuration results is active due to the forward movement of wing location along fuselage as shown in Table 6. The stall speed, take-off and landing distance shows bigger values comparing with a baseline and deterministic configuration results due to the reduction of wing area of RDO configuration results. The horizontal tail root chord and sweep angle variables hit the upper bound for robust design results due to increments in the wing area and wing sweep angle and reduction in the wing location. Hence, the horizontal tail is required to increase a span to satisfy static stability conditions such as the static margin and pitching moment coefficient. The optimum results for vertical tail geometry and its location also satisfy the directional and lateral constraints, as shown in Table 6. The optimum results also recommend flying at a lower speed and altitude to improve the endurance, as shown in the RDO UAV results column. Other performance constraints such as take-off, landing distance, stall speed, maximum speed and lift over drag ratio satisfy the design requirements. The UAV gross, empty and wing weight satisfy the constraints which are set by following a baseline value.

Probabilistic analysis is performed on the deterministic and RDO results considering flight speed and altitude as the noise factor. The results are shown in Fig. 11 and Table 7. The 1,500 sampling points are used for MCS, then the distribution is fitted as shown in Fig. 11. The reason is the central difference method directly used to establish a new RDO objective which needs to run Advanced UAV four times to complete one iteration. In addition, MCS normally requires

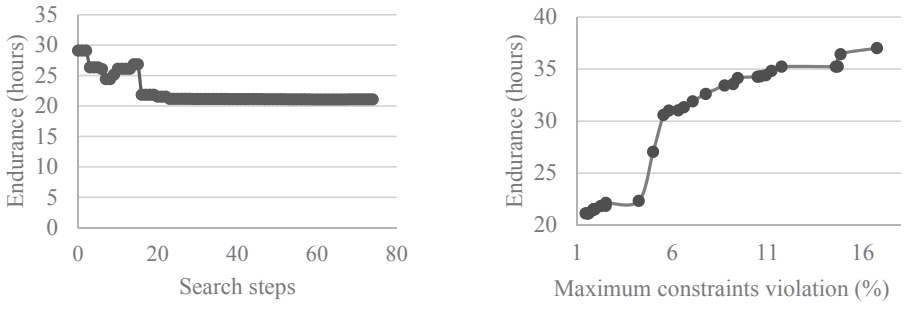
https://doi.org/10.1017/S0001924000009027 Published online by Cambridge University Press

**Table 6**
**MALE UAVs deterministic and RDO design results comparison**

| | | Baseline | Deterministic UAV result | RDO UAV result | Unit |
|---|---|---|---|---|---|
| Objective function | Endurance | 18·6 | 21·13 | 22·19 | hours |
| Design Variables | Wing span | 14·8 | 15·01 | 13·15 | m |
| | Wing root chord | 1·24 | 1·23 | 1·16 | m |
| | Wing tip chord | 0·5 | 0·52 | 0·7 | m |
| | Wing sweep | 5 | 7·85 | 10 | deg |
| | Wing dihedral | 0 | 0 | 0 | deg |
| | Wing location | 3·59 | 3·43 | 3·06 | m |
| | HT span | 4 | 3·51 | 3·94 | m |
| | HT root chord | 0·742 | 0·743 | 1·28 | m |
| | HT tip chord | 0·742 | 0·695 | 0·43 | m |
| | HT sweep | 0 | 10 | 0·87 | deg |
| | HT location | 6·82 | 6·24 | 6·87 | m |
| | VT span | 1·14 | 1·6 | 1·6 | m |
| | VT root chord | 0·742 | 0·958 | 1·07 | m |
| | VT tip chord | 0·742 | 0·77 | 0·95 | m |
| | VT LE sweep | 0 | 6·44 | 3·9 | deg |
| | VT location | 6·82 | 7·8 | 6·56 | m |
| | $V_{design}$ | 42 | 38 | 36·38 | $ms^{-1}$ |
| Constraints | Flight altitude | 3000 | 2754 | 2025 | m |
| | Wing taper ratio | 0·4 | 0·42 | 0·6 | |
| | Lift to drag ratio | 21·3 | 21·55 | 21·07 | |
| | Maximum speed | 64·35 | 64 | 62·3 | $ms^{-1}$ |
| | Stall speed | 24·48 | 24·27 | 25·11 | $ms^{-1}$ |
| | Takeoff ground roll | 387·6 | 381 | 409·3 | m |
| | Takeoff field length | 651·7 | 647·6 | 699·2 | m |
| | Landing distance | 402·7 | 397·8 | 407·79 | m |
| | $C_{lb}$ | 0·0069 | –0·123 | –0·183 | |
| | $C_{nb}$ | 0·0055 | 0·05 | 0·0589 | |
| | $C_{m\alpha}$ | –1·074 | –1·46 | –1·464 | |
| | Static Margin | 0·156 | 0·15 | 0·20 | |
| | Wing weight | 91 | 91 | 89·44 | kg |
| | MTOW | 1011·7 | 1010 | 1009·9 | kg |
| | Empty weight | 334·7 | 333·2 | 332·9 | kg |

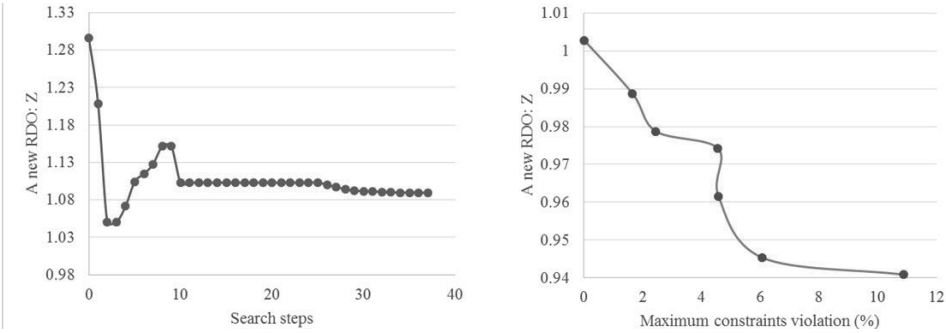
at least one million sampling points to obtain a simulation result. Therefore, the fitting method is applied to generate a fit distribution curve in Fig. 11 while still maintaining the accuracy of probabilistic analysis results and saving MCS runs. The target endurance mean value and target variance value are set as 21 hours and 1·5 hours respectively. The comparison is presented in Table 7, which shows a small improvement in the endurance objective function at 3·46%. However, the variance reduces from 9·57 hours to 1·5 hours with 84·33% improvement which is also seen in Fig. 11, while the RDO fitting distribution provides narrow and more reliable results compared

https://doi.org/10.1017/S0001924000009027 Published online by Cambridge University Press




(a) Convergent history (b) Constraints violation for UAV endurance

Figure 10. Deterministic optimisation results for MALE UAV.




(a) Convergent history (b) Constraints violation for UAV endurance

Figure 11. Robust design optimisation results for MALE UAV.

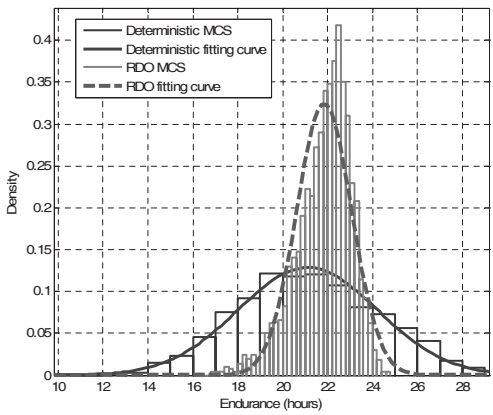



Figure 12. MCS and fitting distribution deterministic results and RDO comparison.

https://doi.org/10.1017/S0001924000009027 Published online by Cambridge University Press

with the deterministic UAV results. The reliability is also increased by 55·56% compared with the deterministic results because the RDO process reduces the sensitivities of the noise factor to the endurance objective function. Therefore, the RDO process demonstrates the improvement of reliability in the UAV performance results while considering the uncertainty parameters and provides trustworthy design results compared with the traditional deterministic design optimisation approach at the conceptual design stage.

The computational strategy for the proposed robust UAV design implements a central difference method and fitting distribution for 1,500 sampling points of MCS, which shows extreme computational time-savings compared with the normal RDO method, which requires at least 1 million sampling points, as shown in Table 8. The central difference finite method directly calculates the differentiation of speed and altitude noise parameters with a small step size for the adjusted variance of response. The MCS sampling points are investigated for a given UAV design application to select 1,500 sampling points based on the distribution fitting tool and distribution history for 500, 1,000 and 1,500 comparison. The computer performance configuration is i7, 3·07GHz and 16GB of RAM with a parallel computing set for 4 CPUs. The proposed UAV RDO framework only requires about 21 hours to obtain probabilistic analysis results compared with the 116 days expected for a normal RDO approach as shown in Table 8. Therefore, the computational strategy for the UAV RDO framework is extremely efficient compared with a normal RDO approach.

**Table 7**
**Comparison of deterministic and robust design results probabilistic analysis**

| | Deterministic results | Robust design results | Improvement (%) | Unit |
|---|---|---|---|---|
| Endurance | 21·11 | 21·84 | 3·46 | hours |
| Variance | 9·57 | 1·5 | 84·33 | hours |
| Probability | ($P_r \geq$ 21hr) | 50·4 % | 78·4% | 55·56 |

**Table 8**
**Comparison of computational strategy of probabilistic analysis for UAV robust framework**

| | Normal RDO (Estimated) | UAV RDO framework |
|---|---|---|
| No· of calls: Advanced UAV | 1 | 5 |
| Execution time (s): Advanced UAV | 40 | 40 |
| Monte Carlo Simulation (MCS) | 1,000,000 | 1,500 |
| Total computation time (hours) | 2,778 | 20·75 |

## 4.4 Validations of deterministic and RDO configuration results

High fidelity analysis ANSYS Fluent 13[18] is used to validate on a baseline, deterministic and RDO optimal configuration results as shown in Fig. 13. The objective function is the UAV endurance. Therefore, the accuracy of lift to drag ratio is significantly required to be validated by using the high fidelity analysis.

https://doi.org/10.1017/S0001924000009027 Published online by Cambridge University Press

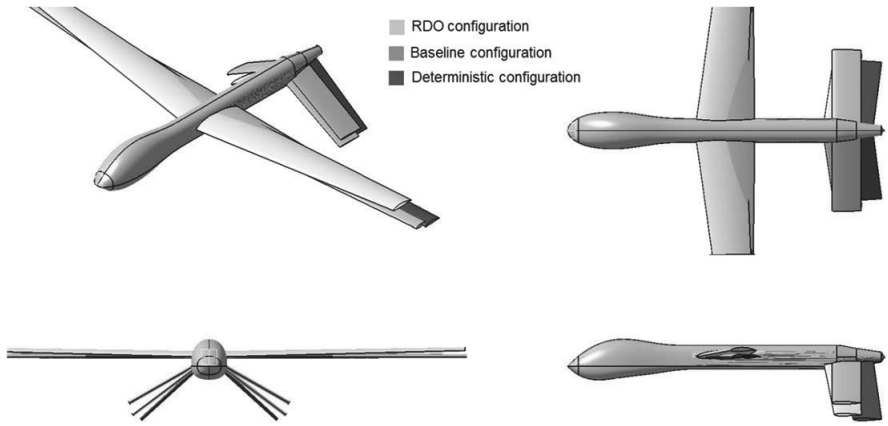



Figure 13. 3D UAV configuration results comparison.

Steady state calculations are used to compute aerodynamic coefficients and flow field of the entire UAV configuration in ANSYS-Fluent 13. The mesh is modeled using Pointwise[23] grid generation software. Reynolds-Averaged Navier-Stokes (RANS) equations are applied to describe flow around UAV Single equation Spalart-Allmaras turbulent model (S-A), which is specifically developed by Spalart and Allmaras for aerospace applications involving wall-bounded flows, is used in current calculation. The model showed a good agreement for boundary layers subjected to adverse pressure gradients.

Flow around half of the entire UAV configuration is investigated due to a symmetric UAV configuration geometry. For precise calculation of boundary-layer properties dense mesh is generated around UAV configuration. Y+ value at wing and tail surface is equal to 1·0 and greater than 1·0 at body surface. Applying Y+ value at the body surface less than 1·0 leads to high aspect ratio cells and mesh geometry problems. Dense mesh with number of grid points of 2·63M is used to precisely predict aerodynamic characteristics of the entire UAV configuration.

Grid topology is shown in Fig. 14. Convergence criteria is selected as the maximum residual of velocity components, energy and continuity less than $10^{-4}$).

The pressure distribution on the entire UAV configuration is displayed in the Fig. 15. The low speed cruise condition is analysed at 42ms$^{-1}$, 38ms$^{-1}$ and 36ms$^{-1}$ for baseline, deterministic and RDO

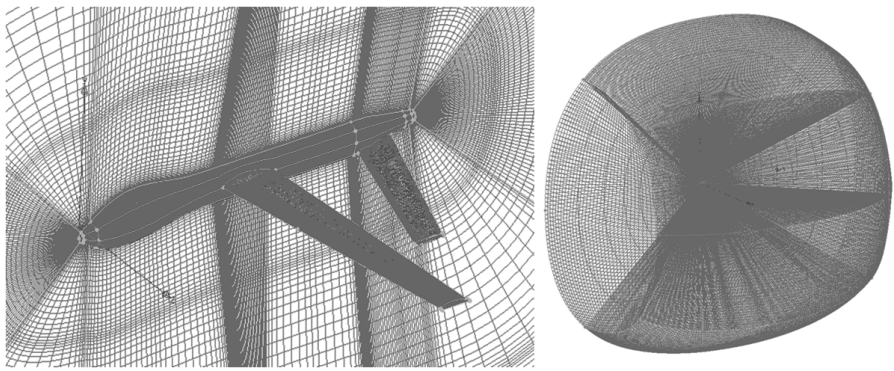


Figure 14. Entire UAV meshing topology grid system.

https://doi.org/10.1017/S0001924000009027 Published online by Cambridge University Press

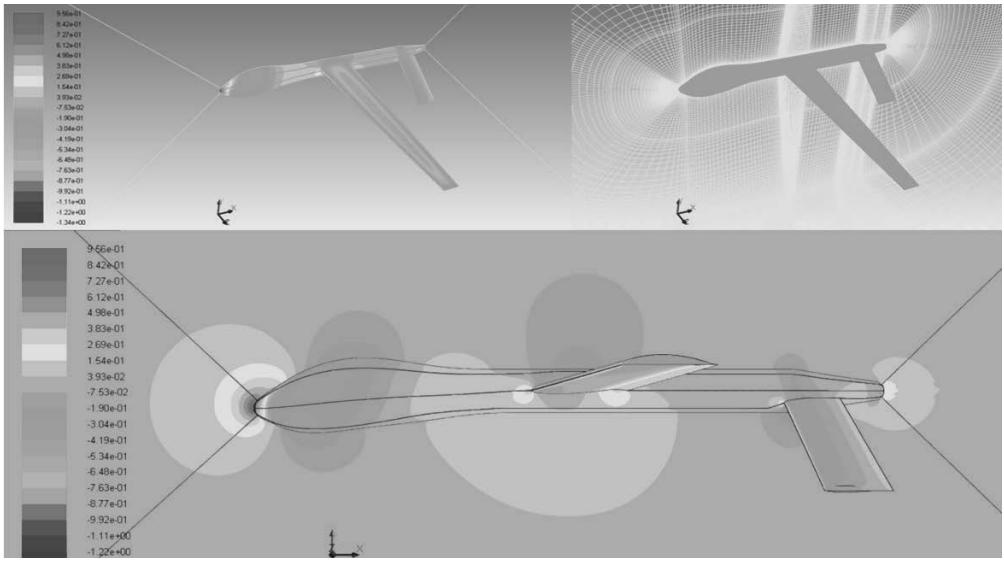



Figure 15. Pressure distribution for the entire UAV configuration.

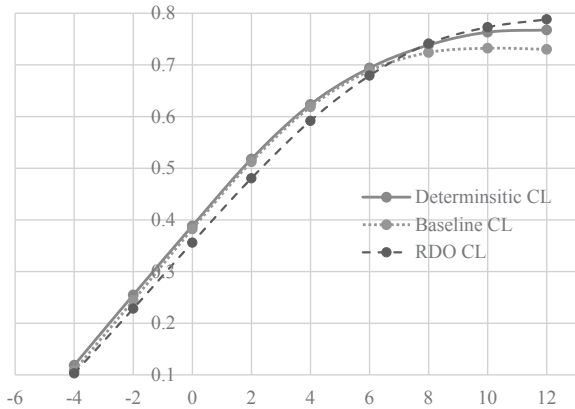



Figure 16. Lift coefficient graphs of ANSYS Fluent 13 results.

configuration, respectively. The highest pressure regions are appeared on the nose of UAV, the lower wing and lower horizontal tail surface as shown on Fig. 15. The lowest pressure region is on the upper wing surface due to very long wing span and low operation speed. Hence, it produces more lift force on the wing and higher lift to drag ratio. The longer endurance is improved. The pressure distribution is higher in the near upper wing tip region due to the induced effect at outboard wing. Therefore, the RANS solver is well-predicted to capture the UAV aerodynamic characteristics. In addition, the turbulence model is applied in the current analysis. However, the flow is low speed regime and mostly laminar in wing, tail and fuselage. Hence, the drag coefficient is over-estimated due to the turbulence model. The baseline, deterministic and RDO configuration are calculated from –4 degree to 10 degree of AoA with the 2 degree of step to build the lift coefficient curve as shown the Fig. 16. The right trend of lift coefficient on the entire UAV configuration are presented.

https://doi.org/10.1017/S0001924000009027 Published online by Cambridge University Press

**Table 9**
**The UAV high fidelity analysis validations comparison**

| | Lift coefficient (Advance UAV tool) | Lift coefficient (ANSYS Fluent 13) | Difference (%) |
|---|---|---|---|
| Baseline configuration | 0·525 | 0·513 | 2·35 |
| Deterministic configuration | 0·528 | 0·518 | 1·91 |
| RDO configuration | 0·493 | 0·480 | 2·54 |

The designed cruise condition of UAV is at 2 degree of AoA. The Advanced UAV tool is validated with ANSYS Fluent 13 for the lift coefficient as shown in Table 9. The validation results shows very close to the high fidelity analysis results at the 2·54% of maximum difference for three UAV configuration.

# 5.0 CONCLUSION

A multidisciplinary robust optimisation framework for UAV conceptual design is developed and applied successfully for improving Predator A endurance with a trustworthy optimum configuration providing a 55·56% improvement in reliability and 84·33% improvement of variance reduction compared with the traditional deterministic approach. The robust optimisation framework demonstrates the effectiveness of reducing the sensitivity of noise factors to an endurance objective function in a UAV conceptual design case study. Especially, the computational strategy for probabilistic analysis shows an extreme computational time-saving compared with the normal RDO approach with the same computer performance.

The Advanced UAV analysis tool is well-suited for multidisciplinary UAV conceptual design and integrated into a robust optimisation framework. Aerodynamics, propeller, weight and performance analysis are validated for a baseline Predator A with a maximum error at 9·28% which is acceptable for the conceptual design stage.

A multidisciplinary UAV design formulation is successfully made for a robust framework which provides a robust optimum UAV configuration without any noticeable increase in design turnaround time in the multidisciplinary design optimisation environment.

The high fidelity ANSYS Fluent 13 is performed on the entire UAV for a baseline, deterministic and RDO configuration. The validation results show a good agreement with the Advanced UAV analysis tool.

# ACKNOWLEDGEMENTS

The authors would like to acknowledge that this research was supported by the 2013 KU Brain Pool (Konkuk University) and the framework of international cooperation program managed by National Research Foundation of Korea (2013K2A1A2054453).

# REFERENCES

1. SOBIESZCZANSKI-SOBIESKI, J. and HAFTKA, R.T. Multidisciplinary aerospace design optimization: survey of recent developments, *Structural and Multidisciplinary Optimization*, 1997, **14**, (1), pp 1-23.
2. MAVRIS, D.N., BANDTE, O. and DELAURENTIS, D.A. Robust design simulation: a probabilistic approach to multidisciplinary design, *J Aircr*, 1999, **36**, (1), pp 298-307.

https://doi.org/10.1017/S0001924000009027 Published online by Cambridge University Press

3. PARK, G.-J., LEE,T.-H., LEE, K.H. and HWANG, K.H. Robust design: An overview, *AIAA J*, 2006, **44**, (1), pp 181-191.
4. DOLTSINIS, I. and KANG, Z. Robust design of structures using optimization methods, *Computer Methods in Applied Mechanics and Engineering*, June 2004, **193**, (23–26), pp 2221-2237.
5. PARK, H.-U., KIM, S.H., LEE, J.-W. and BYUN, Y.-H. Design of Very Light Jet (VLJ) Aircraft Using Robust Design Optimization Approach, in CJK 5th Proceedings, Jeju, S Korea, 2008.
6. CHEN, W., GARIMELLA, R. and MICHELENA, N. Robust design for improved vehicle handling under a range of maneuver conditions, *Engineering Optimization*, February 2001, **33**, (3), pp 303-326.
7. CHEN, W. and LEWIS, K. Robust design approach for achieving flexibility in multidisciplinary design, *AIAA J*, August 1999, **37**, (8).
8. DU, X and CHEN, W. Efficient uncertainty analysis methods for multidisciplinary robust design, *AIAA J*, March 2002, **40**, (3).
9. CHEN, W., ALLEN, J.K.,TSUI, K.-L. and MISTREE, F. A procedure for robust design: minimizing variations caused by noise factors and control factors, *ASME J Mechanical Design*, *J Mech Des,* **118**, (4), pp 478-485.
10. SANDGREN, E. and CAMERON, T.M. Robust design optimization of structures through consideration of variation, *Computers and Structures*, 2002, **80**, pp 1605-1613.
11. ModelCenter 10.1, PHX ModelCenter®: http://www.phoenix-int.com/software/phx-modelcenter.php
12. PARK, H.-U., LEE, J.-W. and BYUN, Y.-H, Development of the Robust Aerospace System Design Process, 21st Canadian Congress of Applied Mechanics, Department of Mechanical & Industrial Engineering, Ryerson University, Toronto, Ontario, Canada, 3-7 June 2007.
13. AZAMATOV, A., LEE, J.-W. and BYUN, Y.-H. Comprehensive aircraft configuration design tool for integrated product and process development, *Advances in Engineering Software*, January 2011, **42**, (1–2).
14. Nguyen, N.-V. An Efficient Multi-Fidelity Approach for the Multi-Disciplinary Aerospace System Design and Optimization, Ph.D thesis, Konkuk University, Seoul, S Korea, 2011.
15. NGUYEN, N.-V., CHOI, S.-M., KIM, W.-S., KIM, S., LEE, J.-W. and BYUN, Y.-H. Multidisciplinary unmanned combat air vehicle (ucav) system design implementing multi-fidelity models, *Aerospace Science & Technology*, 2012, **26**, (1), pp 200-210.
16. BOOKER, A.J., MECKESHEIMER, M. and TORNG, T. Reliability based design optimization using design explorer, *Optimization and Engineering*, June 2004, **5**, (2), pp 179-205.
17. GUNDLACH IV, J.F. Multi-disciplinary design optimization of subsonic fixed-wing unmanned aerial vehicles projected through 2025, Virginia Polytechnic Institute and State University, USA, 2004.
18. ANSYS Fluent 13, ANSYS, Inc., www.ansys.com.
19. HARTMAN, E.P. and BIERMANN, D. The aerodynamic characteristics of full-scale propellers having 2, 3 and 4 blades of Clark y and R.A.F. 6 airfoil sections, NACA-TR-640, USA,
20. Rotax Turbo Charge 914. http://www.rotaxparts.net/scripts/prodView.asp?idproduct=39.
21. RAYMER, D.P. *Aircraft Design: A Conceptual Approach*, 5th ed, AIAA, 2012.
22. MATLAB 2012 toolbox, http://www.mathworks.co.kr/products/matlab/
23. Pointwise 16 User manual: http://www.pointwise.com/


https://doi.org/10.1017/S0001924000009027 Published online by Cambridge University Press